Available online at www.derpharmachemica.com

ISSN 0975-413X
CODEN (USA): PCHHAX

Der Pharma Chemica, 2018, 10(11): 72-82
(http://www.derpharmachemica.com/archive.html)

Picomolar Level Detection of Insulin in Serum Using Pectin Gold Nanocomposite Platform Immunoassay

Kamatchirajan Balaji Viswanath[1*], Narayanaswamy Krithiga[1], Muthunanthevar Vijayan[2], Sheik Mideen A[3], Vairathevar Sivasamy Vasantha[1]

[1]Department of Natural Products Chemistry, School of Chemistry, Madurai Kamaraj University, Madurai, 625 021, India
[2]Central Electrochemical Research Institute, Karaikudi, 630006, India
[3]Department of Chemistry, Sathyabama Institute of Science and Technology, Chennai, India

ABSTRACT

An electrochemical sensor for the detection of insulin was fabricated, using the electrochemically deposited CCLP- Au NPs modified electrode. The morphology and structure of the CCLP- Au NPs are characterized by Scanning Electron Microscopy (SEM), X-ray Diffraction (XRD), UV-Visible spectroscopy (UV-Vis) and Transmission Electron Microscopy (TEM) studies. The building of the immunosensor was evaluated in each and every step by Cyclic Voltammetry (CV) and Impedance spectroscopy (EIS). The electrochemical detection was based on the anti-insulin-HRP (Horseradish Peroxidase) bundled with Au NPs which binds to the immune complex and the response was observed using Hydro Quinone (HQ) and Hydrogen peroxide (H_2O_2) in phosphate buffer electrolyte. From the results, the sensitivity range is from 50 to 556 pM/l and LOD is calculated as 2.14 pM/l (3σ/s). The developed immunoassay has the ability to insulin in human blood serum samples of healthy individuals.

Keywords: Insulin, Hydroquinone, Hydrogen peroxide, Phosphate buffer, Anti-insulin -*HRP*, CCLP-Au NPs.

INTRODUCTION

Diabetes is one of the most prevalent diseases in the world today and has been predicted to rise worldwide from 171 million in 2000 to 366 million in 2030. Insulin is an important polypeptide hormone that regulates the metabolism of glucose in the blood. The human insulin protein is composed of 55 amino acids and has a molecular mass of 58 kDa. The A-chain and a B-chain of the dimer were linked together by disulfide bonds. Insulin's structure varies slightly between species of animals. Porcine insulin and Equine insulin are especially close to the human version and was widely used to treat type 1 diabetics before human insulin could be produced in large quantities by recombinant DNA technologies. High circulating insulin concentrations may be involved in the pathogenesis of hypertension and cardiovascular disease [1-7]. It is a metabolic disease and can be classified into two main types according to the underlying mechanism. Type I develops when the body fails to make enough insulin, and this type of diabetes is also known as insulin-dependent or juvenile diabetes. It is caused by an autoimmune attract that destroys the insulin-producing cells of the pancreas. Type II diabetes (also known as non-insulin dependent or adult-onset diabetes), occurs when the body is unable to use insulin effectively. Both are characterized by high blood glucose levels. Insulin resistance isn't just a blood sugar problem [3-5]. Nowadays doctors seek the importance of insulin in medical problems beyond diabetes. For better management of diabetes; rapid detection of pancreatic islet-cell malfunction; clear definition of hypoglycemia; precise diagnosis of insulinoma; and early prediction of trauma; there is an urgent need to develop diagnostic devices to monitor levels of insulin and glucose simultaneously, or hence, of the insulin/glucose ratio [8-11]. The insulin detection by impedance spectroscopy for real sample using interdigitated graphene oxide modified electrode is applicable and protein biomarker labeled gold electrode offers very less detection limit in nanomolar range [12,13]. Direct oxidation of insulin achieved using nickel nanoparticles coated on indium tin oxide electrodes and ethylene-diamine assisted carbon nanofibers using NaOH. CNT based electrodes and chitosan/CNT has shown its direct oxidation of insulin at +0.8 V and +0.7 V in pH 7.4, while CNT with transition metal oxide composites has shown its insulin direct oxidation at +0.7 V in more basic conditions using NaCl and NaOH [14-21]. Thus the direct oxidation of insulin is limited due to slow kinetics, surface fouling, very low sensitivity and reproducibility at the electrode surface. Thus our aim is to detect insulin in neutral pH which should be applicable in real sample analysis with very high selectivity and free from interferences.

Pectin (poly galacturonic acid) is a water-soluble naturally occurring sugar polymer present in fruits, cell walls of plants are negatively charged, which is highly biocompatible, biodegradable, and nontoxic. Pectin has the ability to form a supramolecular polymer composite which has two

hydroxyl groups and one carboxylic group which is helpful for forming multiple hydrogen bonds and makes it a flexible and robust film. Remarkably, pectin contains -OH and -COOH functional groups which can be used to support the nanoparticles. Pectin is used as a thickening agent in cooking and baking. In manufacturing, pectin is an ingredient in some denture adhesives [22-24]. Recently, Gold nanoparticles (Au NPs) play a predominant role in the development of nanotechnology due to its high stability, biocompatibility, excellent electron conductivity and unique surface chemistry. Specific size and morphology of the Au NPs have been the focus of intensive research because of its potential applications in the field of electronic, optical, optoelectronic and magnetic devices [25,26]. Au-NPs could be prepared using traditional methods and they can be conjugated polymers, surfactants, drugs, DNA, RNA, proteins, peptides and oligonucleotides for several applications. Au NPs binding towards the amino group and enhances as an electroactive label by accelerating the electron transfer. However, here pectin acts as the stabilizing agent in Au NPs and very few reports for chemical synthesis of other nanoparticles. The gold nanoparticle surface can be used for selective oxidation or in certain cases the surface can reduce a reaction. The interaction of serum proteins with Au NPs is becoming an interesting area of research in the field of biosensors. Au NPs binding towards amino group amplifies the electrochemical signal and retains the biological activity of antibody *via* improving the analytical performance of immunoassay [27-32].

Recently, the electrochemical immunoassay based technique has attracted considerable interest for highly sensitive detection of proteins because of its inherent simplicity, low cost, high sensitivity, and miniaturization. After a complete immunoreaction, the activities of captured enzyme labels on the sensor surface were determined electrochemically by measuring its enzymatic product in the presence of substrates. The sensitivities of the sensors are affected by the enzymatic reaction time, temperature and the substrates. More recently, the use of metallic nanomaterial labels including gold nanoparticles**,** semiconductor crystals and apoferritin nanoparticles in electrochemical immunoassay have shown great promise for sensitive detection of proteins [33-35].

In this work, we have developed an immunosensor platform containing CCLP-AuNPs/GCE, which was immobilized with anti-insulin/BSA/insulin film. The electrochemical signaling is due to the presence of HRP tagged in a secondary antibody (Au-anti-insulin-HRP) which gives a redox couple by catalyzing the Hydroquinone (HQ) and Hydrogen Peroxide (HP) in the electrolyte. The step by step modification of our developed immunoassay was confirmed by cyclic voltammetry and impedance spectroscopy studies. Our developed immunoassay is able to detect the insulin in human blood serum at the clinical range. The CCLP-Au NPs film was highly stable because here the calcium cross-linked pectin acts as an excellent stabilizer for the Au NPs. The developed immunoassay has a low detection limit in the picomolar concentration of insulin and highly selective towards insulin compared with other possible interferences.

MATERIALS AND METHODS

Chemicals

Chloroauric acid, Pectin from citrus peel, Hydroquinone, Disodium hydrogen phosphate, monosodium dihydrogen phosphate and bovine serum albumin (BSA) were purchased from Sigma Aldrich, India. Concentrated HCl, H_2O_2 were of analytical grade purchased from Merck, India. Potassium Chloride, Potassium hexacyanoferrate, and Potassium Ferricyanide were of laboratory reagent purchased from Himedia, India. Calcium Chloride (fused) was purchased from Lobachemic India. Monoclonal anti-insulin antibody produced in the mouse was brought from Abcam. The recombinant insulin protein was purchased from Abcam Pvt Ltd. All the reagents used for the experiments were prepared in double distilled water.

Apparatus

Cyclic voltammetry (CV) and Square wave voltammetry (SWV) was carried out with a Biologic Scientific Instrument (SP-150), electrochemical workstation. Electro Impedance Spectroscopy (EIS) was carried out using CHI Instrument (6206e) electrochemical analyzer. Conventional three electrode systems were used at room temperature with glassy carbon electrode (GCE) 3 mm diameter as a working electrode, Ag/Agcl (saturated KCl) is used as a reference electrode and platinum wire as a counter electrode for the present work. Prior to use, the glassy carbon electrode (GCE) was polished by 0.3 μm and 0.05 μm alumina slurry followed by rinsing with water, ethanol, and water, in turn. The 0.1 M phosphate buffer solution (pH 7.0) was used to prepare electrolyte for CV and SWV. Surface morphological study of the film was studied by using SEM (VEGA-3 TESCAN), TEM (TECHNAI), and FESEM (SUPRA 55VP). Indium tin oxide (ITO) thin film coated glass electrodes were used for surface morphological studies. The UV-visible spectroscopy studies were performed using Agilent Technologies (82357B). Measurements of the pH were made with an EUTECH Instrument's pH meter.

Preparation of electrochemical immunosensor assay

First, the CCLP-Au NPs modified electrode was prepared as per the protocol followed in our earlier report [36]**,** In brief, a solution containing 6 mg/ml of $CaCl_2$, 3 mg/ml pectin and 0.1 mM $HAuCl_4$ was prepared and sonicated well for 30 min. The CCLP-Au NPs film was electrochemically deposited from the mixture on glassy carbon electrode by cyclic voltammetric technique between the potential range 1.4 V and -1.2 V for 10 cycles at 50 mV/s (Figure S1). During the forward scan, a cathodic peak was appeared at the potential of +0.40 V which is corresponding to the reduction of Au^{3+} ions on the electrode surface. During beck ward scan, a peak at -0.70 V was appeared due to the evolution of hydrogen leads to generation of OH^- ions at the electrode-electrolyte interface and thus increase pH of the interface to alkaline condition. Hence, pectin has been deposited as gel in the first cycle. In the second cycle, the reduction peak current of Au NPs is doubled with shift in the reduction peak potential to ~350 mV more positive side (+ 0.75 V) which indicating the growth of Au NPs. This catalytic behavior observed in the second cycle must be due to the deposition of Au NPs which is taking place on the pectin modified Au NPs/GCE surface not on the bare GC and thereby decreasing aggregation of gold nanoparticles. Hence, the interaction between –COOH and –OH of pectin with Au^{3+}ions may be leading to preconcentration of Au^{3+} ions in the electrode – electrolyte interface. In the reverse scan, a sharp anodic peak was observed at the potential of + 1.10 V should be ascribed to the oxidation of Au nanoparticles. During the continuous electrochemical cycling process, the growth of the reduction and oxidation peak currents reveals the successful formation of Au NPs Then, the CCLP-Au NPs modified electrode was dried and then anti-insulin was drop cast on CCLP-Au NPs modified electrode and kept for 15 min for drying. The above anti-insulin attached electrode was then treated with 0.1% BSA for 10 min to block the unoccupied sites on the CCLP-Au NPs. Then, the modified film GCE/CCLP-Au NPs/anti-insulin/BSA was drop cast with the protein insulin and incubated for 15 min and rinsed with 0.1 M PB (pH 7.0). Finally, 10 μl of Au tagged anti-insulin-HRP was drop cast onto the GCE/CCLP-Au NPs/anti-insulin/BSA/ Insulin and incubated for 30 min and electrode was washed with 0.1 M PB (pH 7.0) for three times. The sandwich structure of GCE/CCLP-Au NPs/anti-insulin/BSA/Insulin/Au-anti-insulin-HRP was formed. Each and every step of modification was analyzed using PB containing 2.5 mM HQ and 1 mM H_2O_2 as an electrolyte.

Sensor interference, regeneration & reproducibility

The modified electrode GCE/CCLP-Au NPs/anti-insulin/BSA/Insulin/Au-anti-insulin-HRP electrode on treatment with glycine-HCl buffer (100 mM) [pH 2.5] for 10 min removes the antigen and secondary antibody present in it until to get a steady baseline for GCE/CCLP-AuNPs/anti-insulin has been obtained. The above GCE/CCLP-AuNPs/anti-insulin film was stored at 4ºC for further use.

Preparation of Au NPs for anti-insulin tagging HRP

Au-NPs having an average diameter of 10 to 30 nm were prepared by the following method. About 500 µl of 10 mM tetrachloroauric acid aqueous solution was added with 500 µl of an aqueous 10 mM trisodium citrate solution and 18.4 ml of DI water. The freshly prepared 0.1 M $NaBH_4$ solutions (600 µl) in ice cold condition were added to the above solution in stirring condition. The formation of Au NPs was confirmed when the solution turns pink colour immediately. In this reaction, $AuCl_4^-$ is reduced to metallic gold, where BH_4^- acts as the electrons source and the citrate acts as a capping agent for controlling the particle growth. To the above Au NPs solution 10 ng/ml of anti-Insulin tagged with HRP was added and then kept at 4°C for 24 h and then used for further studies.

RESULTS AND DISCUSSION

Characterization of CCLP-Au NPs film and the Au tagged anti-insulin–HRP

Figure 1A shows the UV-visible spectrum of pectin in which has absorption peak for free carboxyl group at 290 nm, which completely disappears after the electrochemical deposition of Au NPs along with pectin and new peak arises at 532 nm confirming the presence of Au NPs [36,37]. The sensitivity of the immunoassay was achieved when the antibody (*anti-insulin*-HRP) was bundled with gold nanoparticles using the protocol from the previously reported literature [38]. Figure 1B shows the UV-Visible spectrum of Au-*anti-insulin*-HRP has two peaks, in which the peak at 280 nm indicates the presence of protein in *anti-insulin* and a sharp surface plasmon resonance peak at 508 nm due to the presence of Au NPs, thus this UV-Visible spectrum confirms the fabrication of Au-*anti-insulin*-HRP. Figure 1C displays XRD patterns which have four diffraction peaks at 2θ angles of 38.3°, 44.46°, 64.78° and 77.96° can be manifested to the (111), (200), (220) and (311) reflections of the face-centered cubic structure of metallic Au NPs in the CCLP-Au NPs film [39-41].

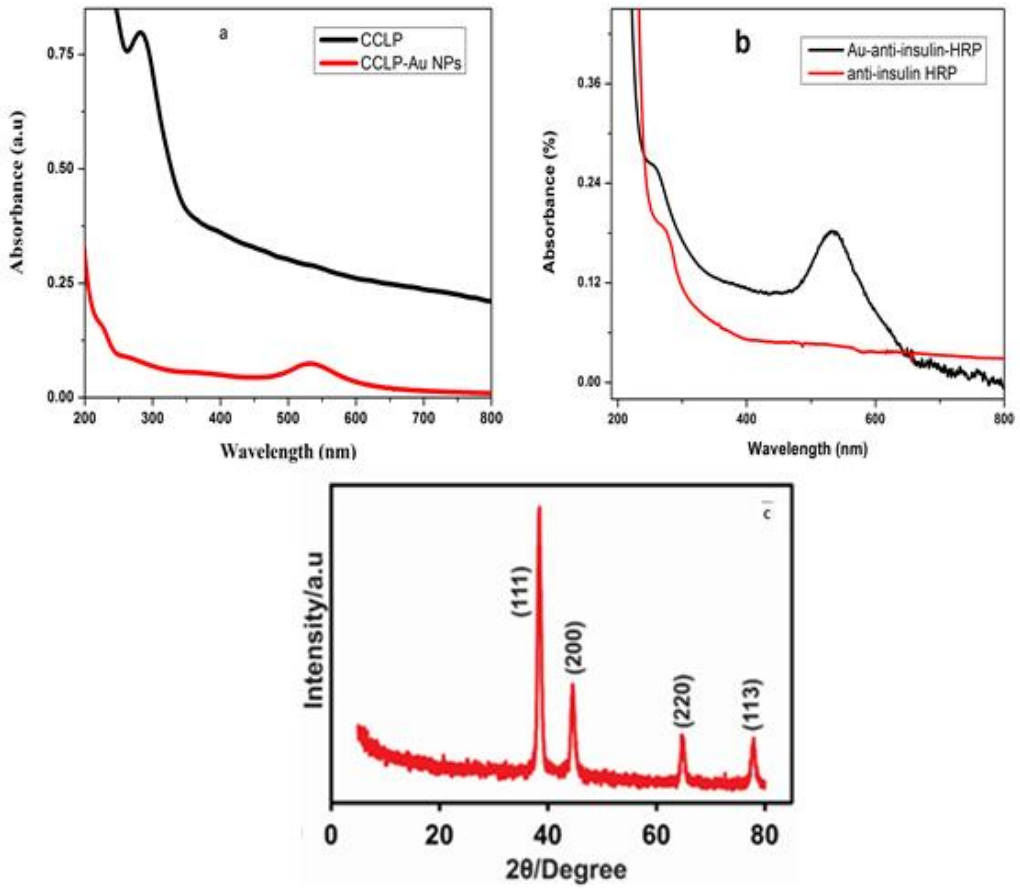

Figure 1: A) UV-Visible spectra analysis of CCLP and CCLP-Au NPs. B) UV-Visible spectra analysis of Anti-insulin-HRP and Au tagged Anti-insulin - HRP. C) XRD pattern of CCLP-Au NPs composite

Figure 2A shows the Scanning Electron Microscopy (SEM) image of Au-Anti-insulin -HRP prepared using a standard protocol, the spherical shaped nanoparticles ranging from 10 to 70 nm were observed. Figure 2B shows the SEM image CCLP-Au NPs composite in which uniform decoration of Au NPs on the calcium cross-linked pectin with the particle size varying from 12 to 50 nm. The EDX spectrum of CCLP-Au NPs composite presents the signals for carbon, oxygen, calcium, and gold with a weight percentage of 15.10, 35.12, 16.08 and 33.70%, respectively (inset to Figure 1B). The presence of a high weight percentage of gold in the EDX spectra indicates the presence of a higher amount of gold nanoparticles into the CCLP matrix. Thus we can confirm that CCLP act as a good stabilizer for the Au NPs. Figure 2C shows the Transmission Electron Microscopy (TEM) image of Au-Anti-insulin -HRP with hexagonal shaped particles ranging from 10 to 30 nm. Figure 2D shows the TEM image of the CCLP-Au NPs found as clustered in nature and the size of the Au NPs very small (i.e.~5 nM). Figure 2E shows the SEM micrograph of the anti-insulin observed at the magnification of 12.4 Kx. Figure 2F shows the FESEM image for the formation of immunocomplex between the insulin protein and the anti-insulin, the binding leads to a change in shape and size was increased from 5 to 7 µm.

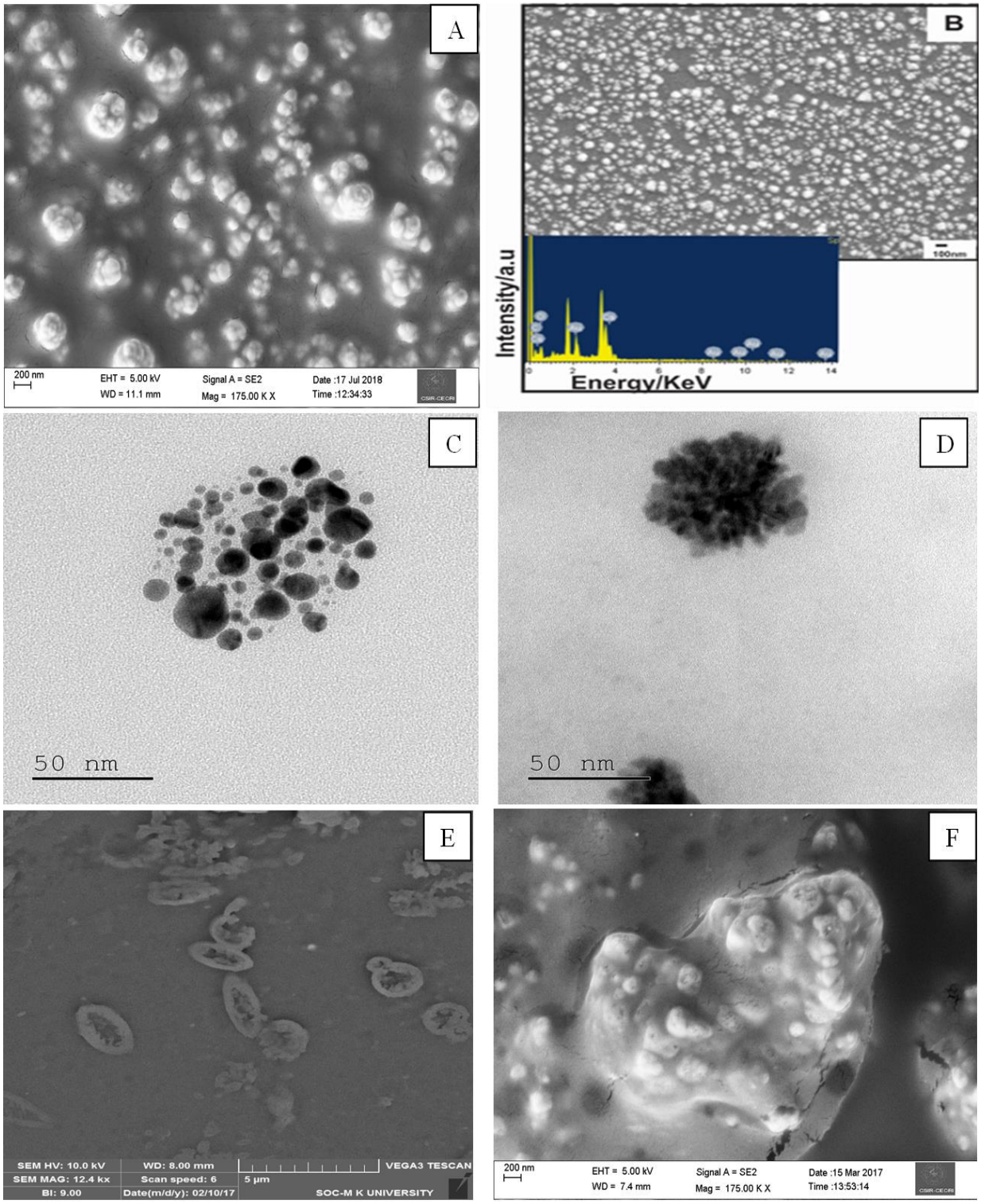

Figure 2: (A) SEM micrograph of Au-Anti-insulin -HRP; (B) SEM image, EDX spectra (inset to Figure 2B) of CCLP-Au NPs film; (C) TEM image of Au tagged-Anti-insulin -HRP, (D) TEM image of CCLP-Au NPs; (E) SEM micrograph for anti-insulin and (F) FESEM Micrograph for Insulin and anti-insulin (immunocomplex)

Optimization of the experimental conditions of the immunoassay

The performance of the electrochemical immunoassay mainly depends on the experimental conditions. The concentrations of HQ, H_2O_2 and Au-Anti-insulin-HRP and the incubation time all play a vital role in the current response of the immunosensor. As shown in Figure 3A**,** under the same concentrations of H_2O_2 and Au-Anti-insulin-HRP and incubation time, the current response of the immunosensor increased with increasing concentration of HQ from 0.5 to 2.5 mM and attained limiting current beyond 2.5 mM. Thus, the optimized concentration of HQ was 2.5 mM. Figure 3B shows the effect of H_2O_2 concentration on the current response of the immunosensor. As the maximum current was obtained at 1.0 mM H_2O_2, it was chosen as the optimum concentration. Then the effect of Au-Anti-insulin-HRP concentration on the catalytic current of the electrochemical immunoassay was studied in the presence of 2.5 mM HQ and 1.0 mM H_2O_2. The catalytic current of the immunoassay increased with increasing concentration of Au-anti-insulin-HRP from 3.5 to 20 ng/ml and a further increase of Au-anti-insulin-HRP concentration had no effect. Thus 10 ng/ml was the optimized concentration of shown in Figure 3C. The effect of incubation time was studied from 20 to 60 min and the results showed that 30 min was the optimum time for getting high catalytic current shown in Figure 3D.

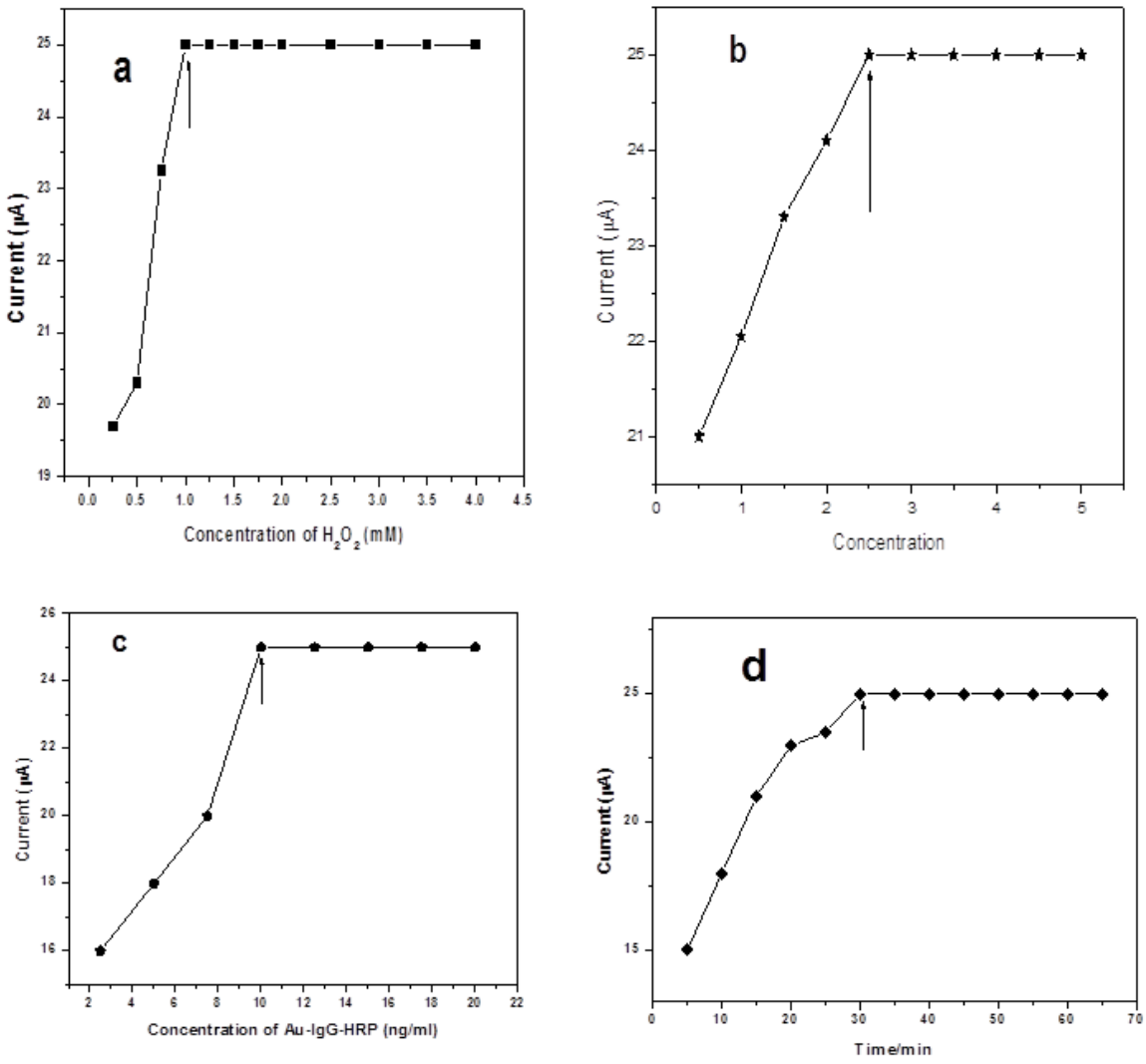

Figure 3: Optimization of the experimental conditions of the immunoassay in PB (pH 7.0) (A) at various concentration of H_2O_2 under 2.5 mM HQ, 18 ng/ml Au-Anti-insulin -HRP and incubation for 30 min; (B) at various concentration of HQ under 1 mM H_2O_2, 10 ng/ml Au-Anti-insulin -HRP and incubation for 30 min; (C) at various concentration of Au-Anti-insulin -HRP under 2.5 mM HQ, 1 mM H_2O_2 and incubation for 30 min; (D) at various incubation time under 2.5 mM HQ, 1 mM H_2O_2 and 14 ng/mL Au-anti-insulin-HRP.

Confirmation of formation of the immunosensor assay by cyclic voltammetry and impedances analysis

Figure 4A shows the Electrochemical Impedance Spectroscopy (Nyquist plots) for bare GCE and surface modified electrodes measured using the electrolyte 5 mM $Fe(CN_6)^{3-/4-}$ in PB at a frequency range between 0.1 Hz and 100 kHz. Bare GCE shows a small semicircle with Rct of 434 Ω (curve 1) while CCLP-Au -NPs/GCE shows Rct of 2079 Ω (curve 2), this confirms that due to the non-conducting CCLP in CCLP-Au NPs film was responsible for the high Rct value even though it has highly conducting Au NPs on it. After, the immobilization of anti-insulin on CCLP-Au NPs/GCE further increases the Rct value to 9050 Ω (curve 3). When the unoccupied sites are blocked with BSA, the Rct value was further increased to 166469 Ω (curve 4). On further addition of the target insulin on CCLP-Au NPs/anti-insulin modified electrode again increased the Rct value as 401461 Ω (curve 5), which confirms the successful immobilization of the poor conducting insulin. Finally, when Au-Anti-insulin -HRP was immobilized on the GCE/CCLP-Au NPs/anti-insulin/BSA/Insulin surface, the Rct value of the above film is decreased to 201109 Ω (curve 6), because the presence of Au NPs in the Au-anti-insulin-HRP makes it conductive in nature [42].

Figure 4B shows the cyclic voltammograms of the above-modified electrodes from -0.3 V to 0.6 V at 50 mV/s using the electrolyte in PB containing 2.5 mM HQ and 1 mM H_2O_2. The CV for bare GCE (curve 1) and all the other modified films shows a redox peak for HQ with hydrogen peroxide as in PB. Then, the CCLP-Au NPs modified electrode was dried at room temperature and subjected to voltammetric studies in PB containing 2.5 mM HQ and 1 mM H_2O_2 (curve 2). Then the anti-insulin was drop cast on CCLP-Au NPs modified electrode and kept at open air for 15 min. Then, the GCE/CCLP-Au NPs/anti-insulin film modified electrode was formed which was confirmed by voltammetric which shows a redox peak with low peak current when compared to CCLP-Au NPs modified electrode (curve 3). Then the prepared GCE/CCLP-Au NPs/anti-insulin treated with 0.1% BSA for 10 min to block the redundant sites on the surface of CCLP-Au NPs (curve 4). Thus, the modified film GCE/CCLP-Au NPs/anti-insulin/BSA was dipped and incubated with the antigen for 15 min and rinsed with 0.1 M PB (pH 7.0). The GCE/CCLP-Au NPs/anti-insulin/ BSA/Insulin modified electrode was formed (curve 5). Then, 10 µl of Au tagged Anti-insulin -HRP was drop cast onto the GCE/CCLP-Au NPs/anti-insulin/Insulin and incubated for 30 min and electrode was washed with 0.1 M PB (pH 7.0) for three times (curve 6). Thus, the sandwich structure of GCE/CCLP-Au NPs/anti-insulin/Insulin/Au-Anti-insulin-HRP film modified electrode was formed. All the above antibody, BSA blocking, antigen and gold tagged antibody loading steps of the modified electrode to voltammetric scanning towards 2.5 mM HQ and 1 mM H_2O_2, in PB, by measuring their changes in the peak current. Meanwhile, for a comparative study between Au-anti-insulin-HRP and anti-insulin-HRP antibody loading on the final step in which the Au tagged anti-insulin -HRP shows the higher current response than the anti-insulin-HRP which can be attributed due to the excellent catalytic activity of HRP along with favorable

conductivity of Au NPs which accelerates the electron transfer of the enzymatic substrate to the electrode. The anodic peak current (Ipa) varying with modified electrodes and change in Rct values are listed in Table S1. These results confirm the formation of a sandwich type of immunoassay.

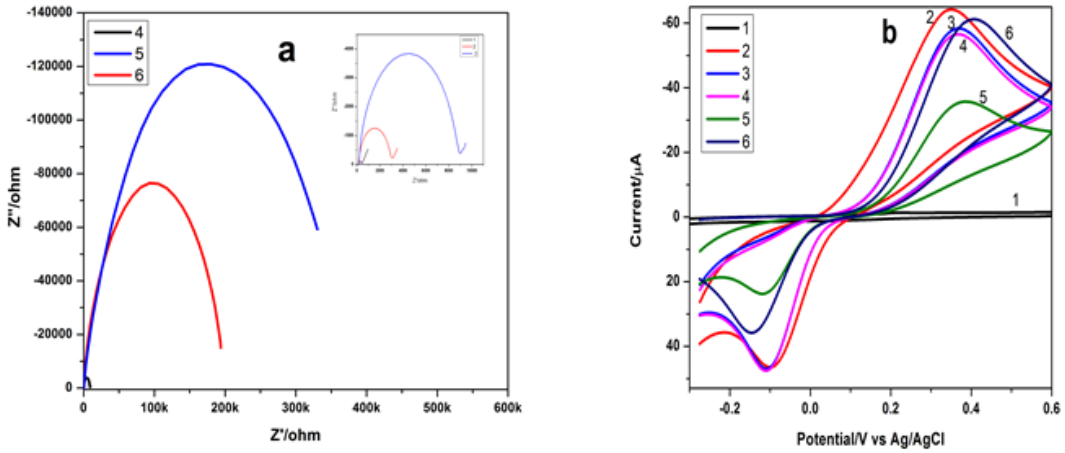

Figure 4: (A) Electrochemical Impedance Spectroscopy of bare GCE (1), CCLP-Au NPs/GCE (2), CCLP-Au NPs/anti Insulin/GCE (3), CCLP-Au NPs/anti Insulin/bsa/GCE (4), CCLP-Au NPs/anti Insulin/bsa/Insulin/GCE (5) and CCLP-Au NPs/anti Insulin/bsa/Insulin/Au-Anti-insulin -HRP/GCE (6) in PB (pH 7.0) solution containing 5 mM $Fe(CN_6)^{3-/4-}$ and 0.1 M KCl at a frequency range between 0.1 Hz and 100 kHz. (B) Cyclic Voltammetric studies for (1) bare GCE in PB (pH 7.0), (2) CCLP-Au NPs/GCE, (3) CCLP-Au NPs/anti Insulin/GCE, (4) CCLP-Au NPs/anti Insulin/bsa/GCE, (5) CCLP-Au NPs/anti Insulin/bsa/Insulin and (6) CCLP-Au NPs/anti Insulin/bsa/Insulin/Au-Anti-insulin -HRP/GCE in PB solution containing 2.5 mM HQ and 1 mM HP (pH 7.0)

Evaluation of the immunosensor

The sandwich electrochemical immunoassay for the detection of Insulin (Scheme 1) was developed in various concentration from 50 pM to 556 pM/l, by square wave voltammetric technique in the electrolyte 2.5 mM HQ and 1.0 mM H_2O_2 in PB (pH 7.0) solution using the film GCE/CCLP-Au NPs/anti-insulin/BSA/Insulin/Au-Anti-insulin-HRP (Figure 5A). The main advantages of our developed immunoassay are CCLP-Au NPs was used to offer a larger specific surface area thus helpful in increasing the immobilization amount of antibody loading, and also it has excellent electrochemical behavior by utilization of Anti-insulin-HRP antibodies attached Au NPs (Scheme S1) ball for the signal generation. Figure 5B shows a linear plot of the current of immunosensor *vs* insulin concentration in the range of 50 to 556 pM/l, which showed a good correlation coefficient of 0.9772 with a linear regression equation Diff(i/A) = 27.20+0.027 [Insulin (pM/l)]. These results indicate that the proposed immunosensor for the detection of Insulin is highly sensitive in nature and the detection limit of the sensor is 2.14 pM/l (3σ/s) which is almost far better and lower that of earlier reports. Table 1 shows a comparison of various techniques sandwich model immune complex film with other techniques [8,12-20].

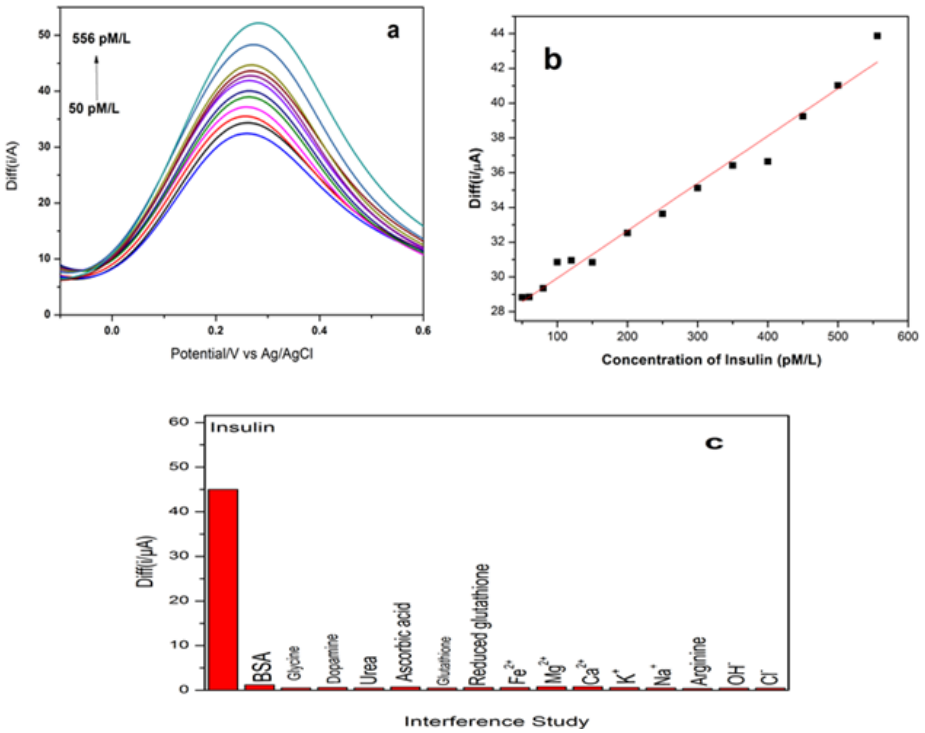

Figure 5: (A) SWV curves in PB (pH 7.0) solution containing 2.5 mM HQ, 1 mM H_2O_2 and various concentrations of insulin at CCLP-Au NPs/anti-insulin/Insulin/Au-Anti-insulin -HRP/GCE; (B) Linear plot for various concentration of insulin ranging from 50 to 556 pM/ml; (C) Interference Study for insulin with various possible interfering substances like aminoacids, biomolecules and essential ions for human body.

Table 1: Comparison of LOD values for our developed electrochemical immunoassay of insulin with earlier reports

Modified Electrode	Technique	LOD	Linear Range	Reference
Gold coated with poly-carboxybetaine methacrylate	Non-faradaic EIS	40 fM	0.1-200 pM	[12]
Reduced graphene oxide modified electrode	EIS	0.086 nM	0.17-172 nM	[13]
MWCNT pyrenebutyric acid	Cyclic Voltammetry	5: 00 PM	8-200 pM	[14]
CNT modified with nickel oxide	Cyclic voltammetry and EIS	6 nM	20-260 nM	[15]
CNT modified with ruthenium oxide	Cyclic voltammetry and amperometry	1 nM	10-800 nM	[16]
Carbon nanofibres modified with nickel oxide	Cyclic Voltammetry	12 nM	20-1000 nM	[17]
Indium tin oxide electrode modified with nickel nanoparticles	Cyclic voltammetry and EIS	10: 00 PM	100-2400 pM & 1-125 nM	[18]
CNT modified with cobalt hexacyanoferrate	Amperometry	40 nM	0.1-3 µM	[19]
Glassy-carbon modified with CNT	Cyclic voltammetry and amperometry	14 nM	50-1000 nM	[8]
Chitosan-CNT	Amperometry	30 nM	0.1-3 µM	[21]
GCE/CCLP-AuNPs/ anti Insulin/Insulin/Au-Anti-insulin - HRP	Square wave voltammetry	2.140 pM/l	50-500 pM/l	This Work

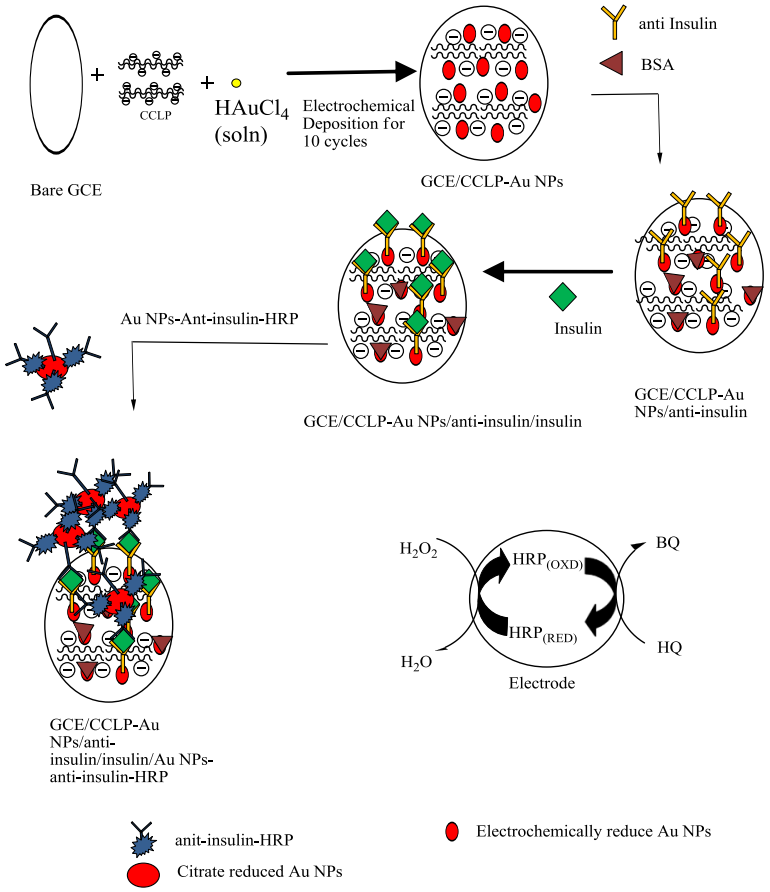

Scheme 1: Graphical abstract for the insulin determination using GCE/CCLP-Au NPs/anti-insulin/insulin/Au-anti-insulin-HRP

Interference study

The selectivity and specificity of the immunoassay was studied using the square wave voltammetry method for several interfering substances including amino acids such as arginine, glutathione, reduced glutathione, glycine, aspartic acid and arginine, most essential ions of our human body such as Na^+, K^+, Ca^{2+}, Mg^{2+}, Cl^-, OH^- and Fe^{2+} and several biomolecules such as dopamine, ascorbic acid, bovine serum albumin were also studied in the same experimental conditions. The fabricated immunosensor doesn't show any interference with the above possible interfering substances as shown in Figure 5C. From all the observed results it clearly shows that the fabricated immunosensor was rapid, specific and selective towards the detection of insulin.

Immunosensor reusability and stability

The regeneration of the immunosenor was essential to reduce the usage of primary antibody (i.e. anti-Insulin) by dissociating the antigen and the immobilized secondary antibody (i.e Au NPs-anti Insulin-HRP). From a study of the literature, glycine·HCl buffer at pH 2.5 was selected as releasing buffer [43,44]. Scheme S2 shows the schematic representation of the reusability procedure. Figures S2-S4 shows the representation of the reproducibility and stability mechanism for the fabricated immunosensor.

Real sample analysis

Human serum samples from two researchers from our own laboratory (Samples 1 and 2) and a farmer (Sample 3) nearby our university was

collected after 30 min of their breakfast and kept at 37ºC for 1 or 2 h and then centrifuged (5 min at 3000 rpm). The usefulness of the developed immunoassay for the analysis of real samples was evaluated by analysis of comparative quantification of the same samples using standard chemiluminescence immunoassay (CLIA) technique also [45]. Thus, the obtained human serum was diluted with sterile phosphate buffer solution in 1:10 ratio and then 5 µl of the diluted serum was added to the GCE/CCLP-Au NPs/anti-insulin/BSA modified electrode and then dried for 20 minutes, and then the Au-Anti-insulin-HRP was drop-casted and then the SWV was measured to find the insulin concentration. Table S2 shows its practical application, the proposed sensor was used to determine insulin from the serum samples. All the real samples show the insulin level in blood serum in an acceptable range according to the standard insulin level chart.

CONCLUSION

A simple and highly sensitive immunosensors was developed based CCLP-Au NPs modified GCE for insulin and each and every step of development of the immunoassay was monitoring using CV and EIS techniques. These experimental results showed that immuno assay has a linear range from 50 to 556 pM/l), lowest detection limit of 2.14 pM/l with good correlation coefficient of 0.98806, good recovery, and high reproducibility for insulin while comparing with the previously reported literatures. In addition, the whole detection time is only 15 min to attain the final step. Consequently, the insulin detection in human serum was also correlated with the performance of the already reported chemiluminescence immonosensors.

ACKNOWLEDGMENT

The corresponding author, V.S. Vasantha, thanks the University Grants Commission (UGC), New Delhi, India [File No. F.41-352/2012 (SR)] by providing the necessary funds to carry out this work. One of the authors Kamatchirajan Balaji Viswanath acknowledges the UGC and Madurai Kamaraj University for the non-NET fellowship.

REFERENCES

[1] J.A. Cox and T.J. Gray, *Anal. Chem.*, **1989**, 61, 2462-2464.
[2] R.T. Kennedy, L. Huang, M. Atkinson, P. Dush, *Anal. Chem.*, **1993**, 65, 1882-1887.
[3] B. Jayaprakasam, S.K. Vareed, L.K. Oslon, M.G. Nair, *J. Agric. Food Chem.*, **2005**, 53, 28-31.
[4] D. Keller, R. Clausen, K. Jofessen, J.J. Led, *Biochemistry*., **2001**, 40, 10732-10740.
[5] T.L. Van Belle, K.T. Coppieters, M.G. Vonherrath, *Physiol. Rev.*, **2011**, 91(1), 79-118.
[6] C.R. Kahn, M.F. White, *J. Clin. Invest.*, **1988**, 82(4), 1151-1156.
[7] V. Singh, S. Krishnan, *Anal. Chem.*, **2015**, 87(5), 2648-2654.
[8] J. Wang, M. Musameh, *Anal. Chim. Acta*., **2004**, 511(1), 33-36.
[9] J.N. Camara, J.T. Suri, F.E. Cappurico, R.A. Wessling, B. Singaram, *Tetrahedron Lett.*, **2002**, 43, 1139-1141.
[10] S. Viswanathan, J.A. Ho, *Biosens. Bioelectron.*, **2007**, 22, 1147–1153.
[11] D.A. Carter, J.D. Wobken, P.K. Dixit, G.A. Bauer, *Exp. Biol. Med.*, **1995**, 209(3), 245-250.
[12] X. Luo, M. Xu, C. Freeman, T. James, J.J. Davis, *Anal. Chem.*, **2013**, 85(8), 4129-4134.
[13] A.K. Yagati, J. Park, S. Cho, *Sensors*, **2016**, 16(1), 109-119.
[14] V. Singh and S. Krishnan, Anal. Chem., **2015**, 87(5), 2648-2654.
[15] B. Rafiee and A.R. Fakhari, *Biosens. Bioelectron.*, **2013**, 46, 130-135.
[16] J. Wang, T. Tangkuaram, S. Loyaprasret, T.V. Alaverz, W. Veersai, P. Kanatharana, P. Thavarungul, *Anal. Chim. Acta*, **2007**, 581(1), 1-6.
[17] L. Zhang, X. Chu, *RSC Adv.*, **2015**, 5(52), 41317-41323.
[18] Y. Yu, M. Guo, M. Yuan, W. Liu, J. Hu, *Biosens. Bioelectron.*, **2016**, 77, 215-219.
[19] F. Qu, M. Yang, Y. Lu, G. Shen, R. Yu, Anal. Bioanal. Chem., **2006**, 386(2), 228-234.
[20] M. Zhang, C. Mullens, W. Gorski, *Anal. Chem.*, **2005,** 77, 6396-6401.
[21] L. Shi, S. Gunasekaran, *Nanoscale Res. Lett.*, **2008**, 3, 491- 495.
[22] B.R. Thakur, R.K. Singh, A.K. Handa, *Crit. Rev. Food Sci.*, **1997**, 37, 47-73.
[23] H. Jonassen, A. Treves, A.L. kjoniksen, G. Smitsad, M. Hiorth, *Biomacromol.*, **2013**, 14, 3523-3531.
[24] J. Shan and H. Tenhu, *Chem. Commun.*, **2007**, 4580-4598.
[25] X. Zhang, Y. Wu, Y. Tu Y and S. Liu, *Analyst*, **2008**, 133, 485-492.
[26] F.T.J. Ngenefeme, N.J. Eko, Y.D. Mbom, N.D. Tantoh, K.W.M. Rui, *Open J. Comp. Mat.*, **2013**, 3, 30.
[27] A. Khazaei, S. Rahmati, Z. Hekmatian, S. Saeednia, *J. Mol. Cat. A: Chem.*, **2013**, 372, 160-166.
[28] H. Kuang, W. Chen, D. Xu, L. Xu, Y. Zhu, L. Liu, H. Chu, C. Peng, C. Xu, S. Zhu, *Biosens. Bioelectron.*, **2010**, 26, 710-716.
[29] B. Kavosi, R. Hallaj, H. Teymourian, A. Salimi, *Biosens. Bioelectron*., **2014**, 59, 389-396.
[30] A. Ambrosi, A. Federico, A. Merkoci, *Anal. Chem.*, **2010**, 82, 1151-1156.
[31] X. Lv, W. Ge, Q. Li, Y. Wu, H. Jiang, X. Wang, *ACS. Appl. Mater. Interfaces.*, **2014**, 6, 11025-11031.
[32] K.M. Pondman, A.W. Maijenburg, F.B. Ceikkol, A.A. Pathan, U. Kishore, B.T. Haken, J.E.T. Elshof, *J. Mater. Chem. B.*, **2013**, 1, 6129-6136.
[33] M.B. Gonzalez-Garcia, C. Fernandez-Sanchez, A.Costa-Garcia, *Biosens. Bioelectron.*, **2000**, 15, 315.
[34] G. Liu, J. Wang, S. Lea, Y. Lin, *Chem. Biochem.*, **2006**, 7, 1315-1319.
[35] D. Rajkumar, V. Mani, S.M. Chen, K. Balaji Viswanath, V.S. Vasantha, M. Govindhasamhy, *RSC Adv*., **2014**, 4, 55900-55907.
[36] X. Kang, G. Pang, Q. Chen, X. Liang, *Sens. Actuators, B.*, **2013**, 177, 1010-1016.
[37] X. Fang, M. Han, G. Lu, W. Tu, Z. Dai, *Sens. Actuators, B.*, **2012**, 168, 271-276.
[38] L. Zheng, L. Jia, B. Li, B. Situ, Q. Liu, Q. Wang, N. Gan, *Molecules.*, **2012,** 17, 5988-6000.
[39] J. Heo, D.S. Kim, Z.H. Kim, Y.W. Lee, D. Kim, M. Kim, K. Kwon, H.J. Park, W.S. Yun, S.W. Han, *Chem. Commun.*, **2008**, 0, 6120-6122.
[40] M.A. Ali, T.A.S. Eldin, G.M.E. Moghazy, I.M. Tork, I.I. Omara, *Int. J. Curr. Microbiol. App. Sci.*, **2014**, 3, 697-708.
[41] M. Iosin, P. Baldeck, S. Astilean, *J. Nanopart. Res.*, **2010**, 12, 2843-2849 (2010).
[42] A.J. Bard, L.R. Faulkner, Electrochemical Methods: Fundamentals and Applications, Wiley New York, **1980**, 2.
[43] S. D. Soelberg, R.C. Stevens, A.P. Limaye, C.E. Furlong, *Anal. Chem.*, **2009**, 81, 2357-2363.
[44] D. Maraldo, K. Rijal, G. Campbel, R. Mutharasan, *Anal. Chem.*, **2007**, 79, 7636-7644.
[45] H.B. Carslake, G.L. Pinchbeck, C.M. Mcgowman, *J. Vet. Intern. Med.*, **2017**, 31, 568-574.

SUPPLEMENTARY INFORMATION

Preparation of Secondary antibody- HRP labeled Au NPs

The commercial form of antiinsulin HRP was diluted to 100 fold in PB from the stock (1: 100 dilution) then solution of 0.5 µl secondary antibody was added to 1.0 ml of gold nanoparticles suspension adjusted to pH (7.0) and stirred effectively for 30 min and kept overnight at 4°C to allow complete coupling of the antibody with gold nanoparticles. After this process, 50 µl of blocking buffer was added on the immunoassay to block the uncoated gold nanoparticles surface and kept at room temperature for 15 min. After coupling, the HRP conjugated secondary antibody coupled with gold nanoparticles was collected by centrifugation (12000 rpm for 15 min at 4ºC). The pellet was dispersed in 1 ml of preservative buffer solution pH 7. After mixing for few 30 min, the suspension was centrifuged again and the pellet was dispersed in 200 µl of preservative buffer and kept for further use. The obtained suspension was further aliquoted to yield 1: 750, 1: 1000, and 1: 5000 dilutions. Before anti insulin conjugated HRP (genei, India) coupled with gold nanoparticle surface, the salt induced aggregated analysis was performed to evaluate the optimum pH 7 used for the conjugation. The color change was observed and it showed an UV-visible spectroscopy absorbance peak at 520 nm which confirms the formation of gold nanoparticles.

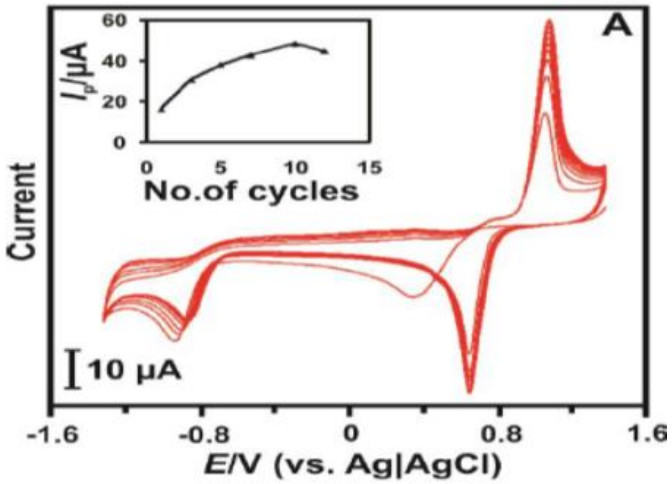

Figure S1: Electrochemical deposition of CCLP-Au NPs by cyclic voltammogram using 6 mg/ml of $CaCl_2$ and 3 mg/ml of pectin and 0.1 mM of HAuCl4 at scan rate of 50 mV/s for 10 cycles

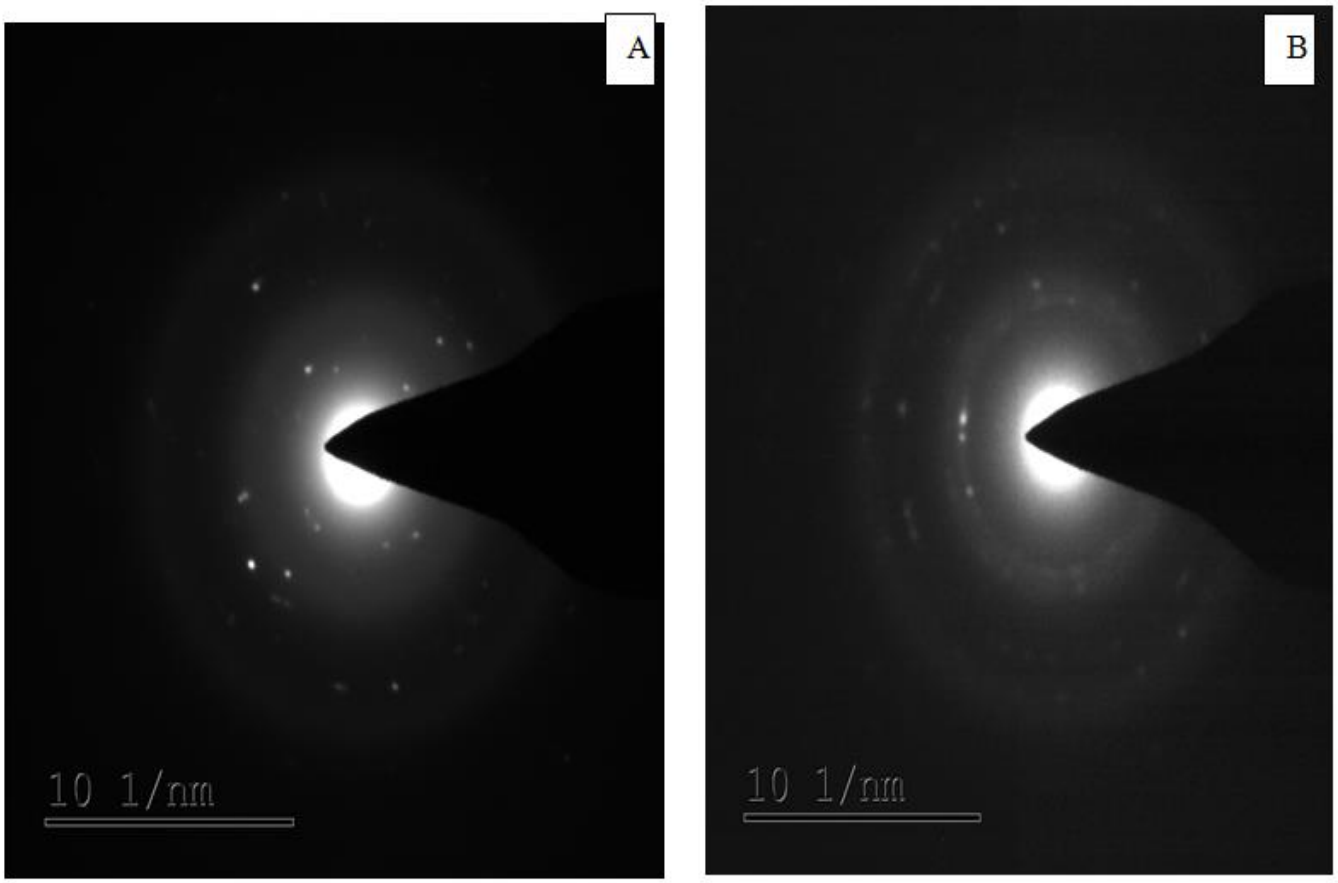

Figure S2: SAED pattern for CCLP-Au NPs (A) and Au-Anti-insulin -HRP (B)

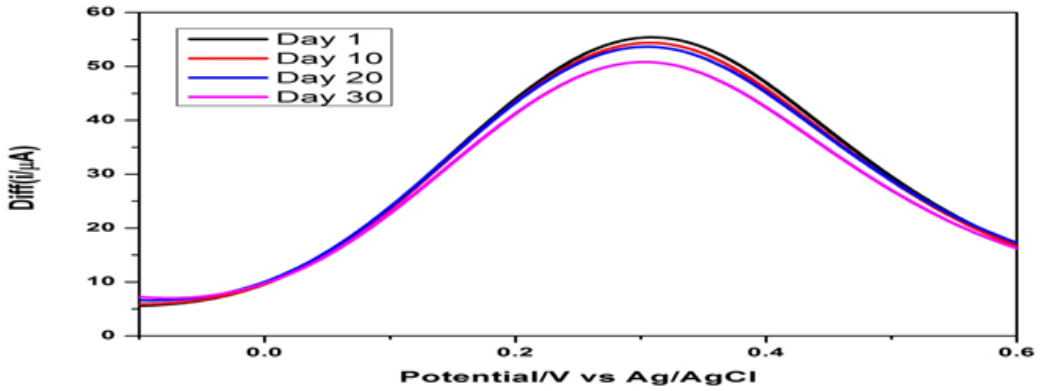

Figure S3: Representation of the reproducibility and stability for the fabricated immunosensors

Modified Electrodes	Ipa (μA)	Rct (Ω)
Bare GCE	0	434
GCE/CCLP-Au NPs	35	2079
GCE/CCLP-Au NPs/anti-insulin	22	9050
GCE/CCLP-Au NPs/anti-insulin/BSA	19.3.	166469
GCE/CCLP-Au NPs/anti-insulin/BSA/insulin	18.8	401461
GCE/CCLP-Au NPs/anti-insulin/BSA/insulin/Au-anti-insulin-HRP	25	201109

Table S1: Tabulated values of anodic peak current and charge transfer resistance of modified electrode surfaces

Sample number	Insulin concentration (pM/l)		Recovery (%)
	The immunosensor	Chemiluminsence	
1	375 ± 0.25	374 ± 0.32	99.75
2	390 ± 0.31	388 ± 0.35	99.49
3	190 ± 0.32	189 ± 0.25	99.43

Table S2: Comparison of insulin detection in serum samples between the developed immunoassay and standard chemiluminsence technique

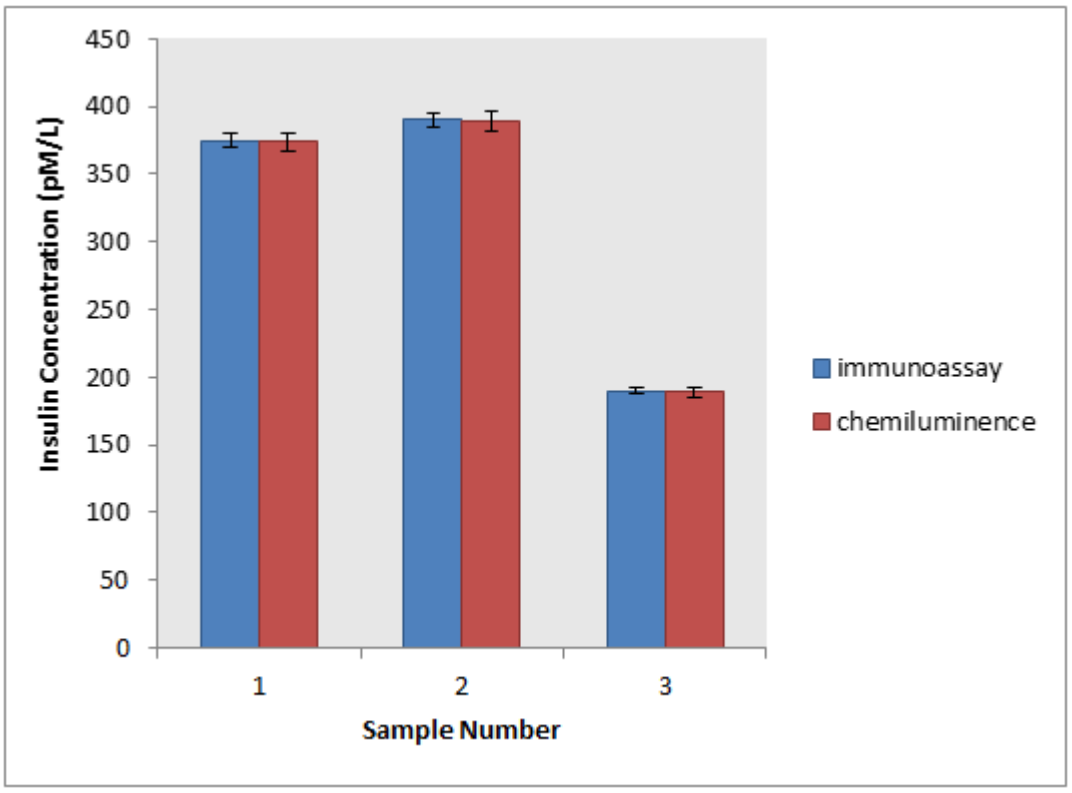

Figure S4: Statistical representation of difference between the two techniques for real sample analysis of insulin

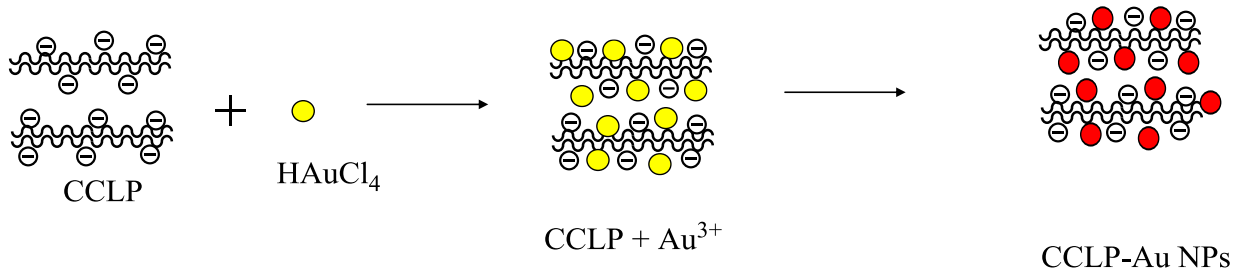

Scheme S1: Preparation of CCLP stabilized Au nanoparticles

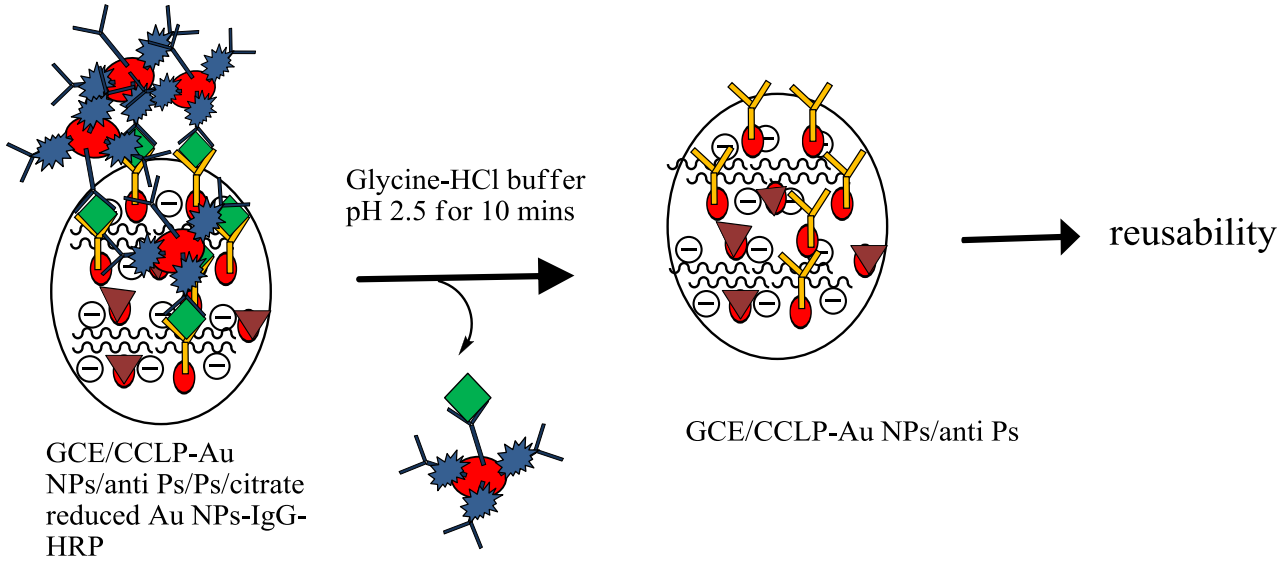

Scheme S2: Schematic representation of the reusability procedure